HIGHLIGHTS FROM THE STAR EXPERIMENT AT RHIC*

Sonia Kabana

for the STAR Collaboration

SUBATECH — Laboratoire de Physique Subatomique
et des Technologies Associees
4 rue Alfred Kastler, 44307 Nantes, France

(Received January 13, 2012)

Experiments using heavy ion collisions at ultrarelativistic energies aim to explore the QCD phase transition and map out the QCD phase diagram. A wealth of remarkable results in this field have been reported recently, for example the Υ suppression discovered recently. We discuss recent results from the STAR experiment focusing on strangeness, charm and beauty production.

DOI:10.5506/APhysPolB.43.535
PACS numbers: 25.75.–q, 25.75.Ag, 25.75.Cj, 25.75.Dw

1. Introduction

Experiments studying heavy ion collisions at ultrarelativistic energies aim to reproduce and study in the laboratory one of the anticipated phase transitions of the early universe, namely the QCD phase transition between partons and hadrons predicted by lattice QCD at a critical temperature of 160–180 MeV and to map out the QCD phase diagram.

The STAR experiment at RHIC with the help of recent important upgrades, including a full-barrel Time-of-Flight (TOF) detector allowing for better particle identification, an upgraded DAQ and implementation of a High Level Trigger (HLT) system, has been able to accumulate a vast amount of high quality data from $p+p$ and Au+Au collisions. In addition, STAR has taken data of Au+Au collisions performing a low energy scan covering the $\sqrt{s_{NN}}$ of 7.7 to 39 GeV, aiming to discover a possible critical point, to study with precision the phase transition characteristics, and map out

* Presented at the Conference "Strangeness in Quark Matter 2011", Kraków, Poland, September 18–24, 2011.

the phase diagram of QCD. In this paper, we present highlights from recent results of the STAR experiment, with a main focus on strangeness, charm and beauty production.

2. Charm and beauty

Open beauty (B) and charm (C) are prominent probes of the sQGP medium produced in central ultrarelativistic heavy ion collisions. STAR is the only experiment at RHIC able to measure charm through direct charmed particle identification in addition to the measurement of charm and beauty through electrons originated from their decays. Electrons are identified using the dE/dx information measured with the Time Projection Chamber (TPC), the information of the electromagnetic calorimeter at high p_{T}, and using the new TOF detector at low p_{T}. These detectors cover the midrapidity region and full azimuthal angle.

The charm cross section at midrapidity has been measured by STAR in a large variety of collisions ($p+p$, d+Au, Cu+Cu, Au+Au) and was found to scale with the number of binary collisions indicating production through initial hard scattering [1]. Beauty and charm cross sections have been measured in $p+p$ collisions at 200 GeV and were found consistent with FONLL calculations [2]. New results show that the beauty contribution to non-photonic electrons in $p+p$ collisions at 500 GeV is more than 60% at p_{T} higher than 8 GeV/c [3].

One way to quantify nuclear effects like the jet quenching is by using the nuclear modification factor R_{AA}. The R_{AA} of fully reconstructed D^0 mesons, measured recently for the first time at RHIC, is shown in Fig. 1 (left panel) to be consistent with 1, namely with no suppression for $p_{\mathrm{T}} < 3$ GeV/c, reflecting the binary scaling behaviour of the charm production cross section [1]. The prediction of a blast-wave fit using the freeze-out parameters of light-quark hadrons (Fig. 1 (left panel)) does not describe the R_{AA} of D^0 mesons, which may indicate that D^0 mesons freeze-out earlier than light-quark hadrons [1]. In the high p_{T} range, a suppression of electrons from open heavy flavour decays appears prominently, in particular, the R_{AA} of electrons from beauty as well as from charm meson decays at $p_{\mathrm{T}} > 5$ GeV/c have been measured to be both significantly suppressed at the 90% confidence level, in central Au+Au collisions at 200 GeV [4].

Quarkonia can be suppressed by colour screening in the plasma, and different states have different dissociation temperatures. The hierarchy of the suppression pattern of quarkonia can therefore serve as a QGP signature and as a thermometer of the quark-gluon plasma formed in these collisions. Also, effects other than colour screening can contribute to the suppression of quarkonia, like *e.g.* suppression by hadronic comovers. In addition, quarkonia can be regenerated from $q\bar{q}$ pairs counteracting a possible suppression.

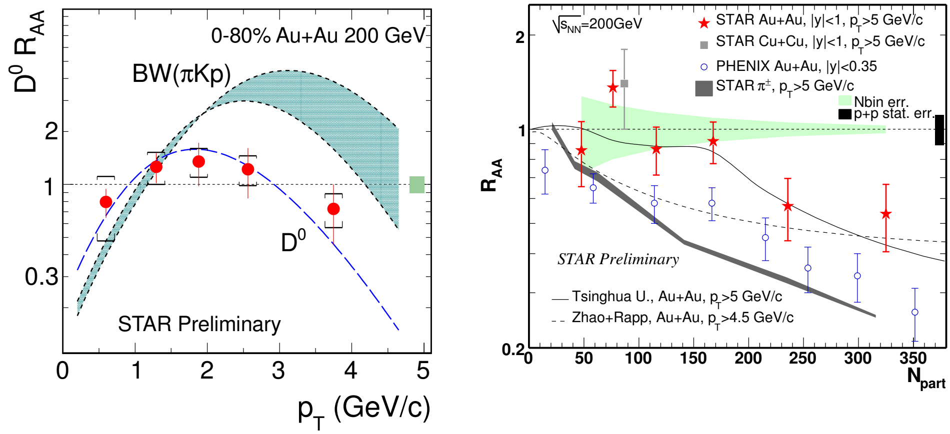

Fig. 1. Left panel: Fully reconstructed D^0 nuclear modification factor R_{AA} as a function of p_{T} in Au+Au collisions at $\sqrt{s_{NN}} = 200$ GeV. The dashed curve shows a blast-wave fit [1]. The shaded band is the predicted D^0 R_{AA} with blast-wave parameters from light-quark hadrons. Right panel: R_{AA} *versus* N_{part} for J/ψ at high $p_{\mathrm{T}} > 5$ GeV$/c$ (stars for Au+Au and one grey rectangle for Cu+Cu collisions) and J/ψ at low $p_{\mathrm{T}} = 0$–5 GeV$/c$ in Au+Au collisions (open circles) measured by PHENIX, and high p_{T} pions (dark thick line). The solid and dashed thin lines show two theoretical calculations (see [5] for details).

The J/ψ has been measured by STAR at midrapidity up to p_{T} of 9 GeV$/c$ in Au+Au collisions, and up to p_{T} of 14 GeV$/c$ in $p+p$ collisions. The R_{AA} factor for the J/ψ has been found to be suppressed in central Au+Au collisions at $p_{\mathrm{T}} > 5$ GeV$/c$, while it exhibits a larger suppression (a smaller R_{AA}) at smaller p_{T} (shown by the open circles measured by PHENIX) (Fig. 1 (right panel)) [5]. The J/ψ measurement in peripheral Au+Au collisions is consistent with previous STAR measurement in Cu+Cu collisions at the same p_{T} and at the same number of participant nucleons (Fig. 1 (right panel)) [6]. The J/ψ measured by STAR at $p_{\mathrm{T}} > 5$ GeV$/c$ and in central Au+Au collisions is less suppressed than the J/ψ measured by CMS in Pb+Pb collisions at $\sqrt{s} = 2.76$ TeV at $p_{\mathrm{T}} > 6.5$ GeV$/c$ and also at midrapidity [7]. This is consistent with a larger system size at the LHC. However, cold nuclear matter effects have to be quantified with d+Au and p+Au collision data as a function of the rapidity and p_{T} to systematically understand the J/ψ production in heavy ion collisions. For a discussion of the J/ψ suppression at low p_{T} at RHIC and LHC please see [8].

Also a different amount of J/ψ regeneration at RHIC and LHC energies would influence the J/ψ energy dependence. STAR has measured the elliptic flow of J/ψ (Fig. 2 (left panel)) to be consistent with zero in the p_{T} range 2 to

8 GeV$/c$ in mid-central Au+Au collisions at 200 GeV [9]. This measurement disfavours J/ψ production dominantly through coalescence from thermalized c and $\bar{c}$ at RHIC, assuming that charm quarks exhibit elliptic flow.

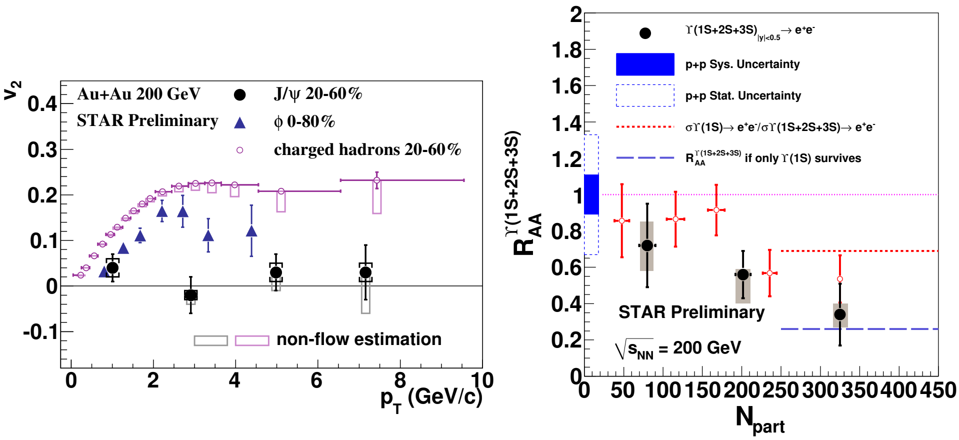

Fig. 2. Left panel: v_2 as a function of p_{T} for J/ψ as well as charged hadrons and ϕ meson in mid-central Au+Au collisions at $\sqrt{s_{NN}} = 200$ GeV. Right panel: R_{AA} of $\Upsilon(1S + 2S + 3S)$ states as a function of the number of participants in Au+Au collisions at $\sqrt{s_{NN}} = 200$ GeV. The solid black points are the Υ results, the open (red) points are the high $p_{\mathrm{T}} > 5$ GeV$/c$ J/ψ results. The black (blue) boxes at (0,1) represent the systematic and statistical uncertainty from the $p+p$ cross section applying to all shown Υ points, while the grey boxes around the Υ points are the systematic uncertainties from other sources (see [10] for details). The dotted (red) line is the ratio of the total cross section of $\Upsilon(1S)$ over the $\Upsilon(1S + 2S + 3S)$. The dashed (purple) line is the ratio of only the direct $\Upsilon(1S)$ cross section over the total $\Upsilon(1S + 2S + 3S)$.

The p_{T} dependence of J/ψ in $p+p$ collisions at 200 GeV extended to low p_{T} through the new TOF detector of STAR can constrain J/ψ production models and data indicate agreement with the Colour Evaporation Model (CEM) at low p_{T} [11]. New results on the p_{T} dependence of the J/ψ polarization in $p + p$ collisions at 200 GeV are consistent with no polarization within uncertainties [12].

Furthermore, STAR has measured the suppression of Υ states $(1S+2S+3S)$ (Fig. 2 (right panel)) in central Au+Au collisions at 200 GeV for the first time at RHIC [10]. This suppression is consistent with suppression of the $2S$ and $3S$ Υ states and only the $1S$ Υ state surviving. This hierarchy of suppression is expected within a colour screening scenario due to the higher dissociation temperature $T_{\mathrm{dissociation}} > 4T_{\mathrm{critical}}$ of the $\Upsilon(1S)$

state [13]. An indication of a suppression of the $(2S+3S)$ Υ states over the $1S$ Υ state suppression has been also observed in Pb+Pb over $p+p$ collisions at the LHC [14].

3. Antimatter and dileptons

STAR has reported recently in a publication in *Nature* the first observation of antihelium-4 [15]. The antihelium-4 yields measured are important for background estimates of antimatter in space. This result has been made possible with the help of the new TOF detector and a High Level Trigger (HLT) in addition to the STAR TPC.

Further results of STAR using the TOF detector involve the measurements of the dilepton invariant mass. These measurements offer access to the in-medium modification of vector mesons in the low mass region (< 1.1 GeV) that could give informations related to the chiral symmetry restoration, while dileptons from thermal QGP radiation and possible modification of correlated charm can be studied in the intermediate mass region (1.1–3 GeV). The dilepton measurement in central Au+Au collisions (Fig. 3 (left panel)) indicates modifications observed in the low and intermediate mass region, when compared to hadronic cocktail simulations [16].

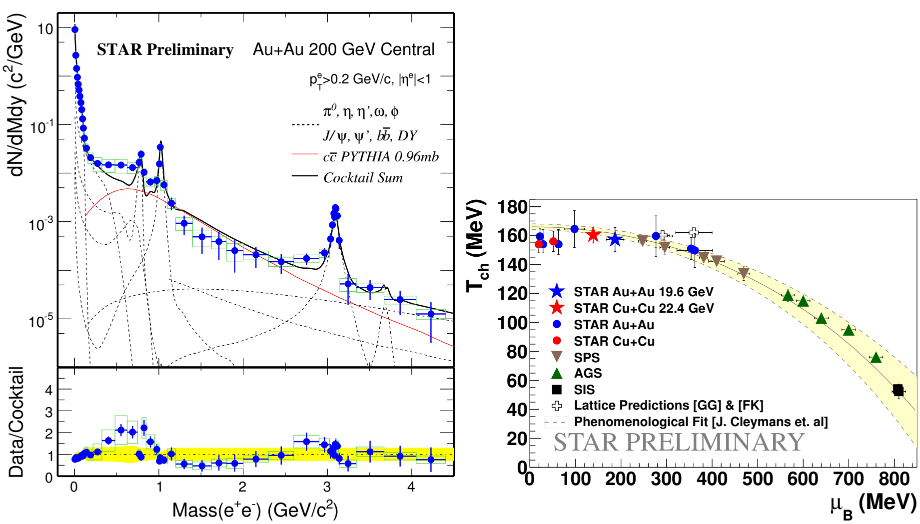

Fig. 3. Left panel: Invariant mass spectra $m(e^+e^-)$ from central Au+Au collisions at $\sqrt{s_{NN}} = 200$ GeV. The grey (yellow) band is the systematic error estimate on the cocktail. Right panel: Temperature as a function of the baryochemical potential both at chemical freeze-out extracted from data of several collision systems together with model predictions and fits.

New results on the ϕ meson indicate that the $\phi \to e^+e^-$ result is consistent with the previous $\phi \to K^+K^-$ result, while no mass shift or width broadening except for known detector resolution effects are observed [17].

4. Beam energy scan

The goal of the Beam Energy Scan (BES) established at RHIC is to measure with precision the critical parameters of the phase transition, and to discover a possible critical point and map out the QCD phase diagram [18]. The collision systems discussed here are Au+Au at $\sqrt{s_{NN}} = 7.7$, 11.5, 19.6, 39, 62.4 and 200 GeV and Cu+Cu at 22.4 GeV. Figure 3 (right panel) shows the points measured by STAR representing the temperature (T(chem)) and baryochemical potential (μ_B(chem)) at the time of chemical freeze-out [19]. The T(chem) and μ_B(chem) parameters have been obtained with a thermal model fit to particle ratios measured at each energy.

A variety of strange particles, in particular Λ, $\overline{\Lambda}$, Ξ^- and $\overline{\Xi}^+$ [20] and kaons [21] have been reconstructed in Au+Au collisions at $\sqrt{s_{NN}} = 7.7$ GeV, 11.5 GeV and 39 GeV using the STAR TPC. Antibaryon to baryon ratios and yields agree well with NA49 data at comparable energies. The μ_B(chem) in $A+A$ collisions has been found to decrease with increasing collision energy, while the T(chem) is found to increase with increasing collision energy and saturate after the region around $\sqrt{s_{NN}} = 10$ GeV [21]. The energy dependence of the strange particle ratios to pions shown in Fig. 4 reflects the above collision energy dependence of T(chem) and μ_B(chem) [21], showing maxima at low energies for the strange particles produced also by associated

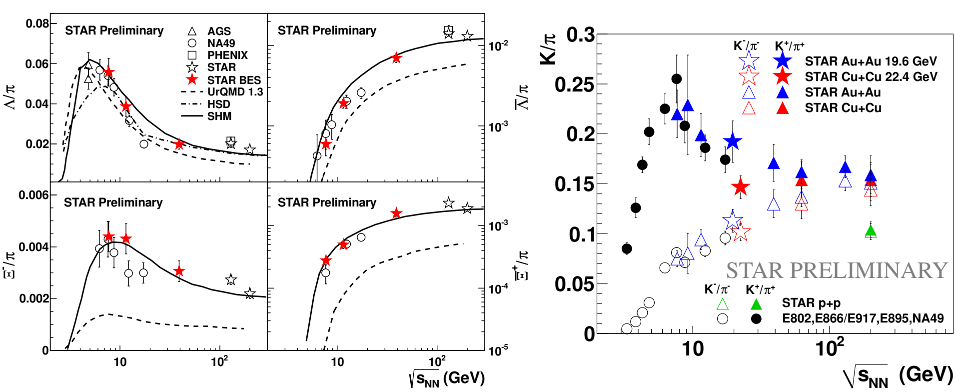

Fig. 4. Left panel: Ratios of Λ, $\overline{\Lambda}$, Ξ^- and $\overline{\Xi}^+$ to pions in central Au+Au and Pb+Pb collisions as a function of $\sqrt{s_{NN}}$ together with model predictions. Right panel: K/π ratio *versus* $\sqrt{s_{NN}}$ for the SIS, AGS, SPS and STAR data including the Beam Energy Scan.

baryon-meson production *e.g.* ΛK^+ [20, 21]. This is expressed also by the agreement of the Statistical Hadron gas Model (SHM) predictions [22] with the data across the whole energy range from AGS to top RHIC energies, shown in Fig. 4 (left panel). This agreement indicates also the applicability of the grand canonical ensemble assumed in this model, to the chemical freeze-out conditions of $A+A$ collisions in a large range of energies.

The nuclear modification factor of the ϕ meson in central with respect to peripheral Au+Au collisions at $\sqrt{s_{NN}} = 39$ GeV has been measured to show no significant suppression up to $p_{\mathrm{T}} = 5$ GeV/c [23]. The elliptic flow coefficient v_2 of ϕ meson, measured up to $p_{\mathrm{T}} = 2$ GeV/c at $\sqrt{s_{NN}} = 11.5$ GeV, shows a deviation from the v_2 of other hadrons in Au+Au collisions at $\sqrt{s_{NN}} = 11.5$ GeV (Fig. 5) [24, 25].

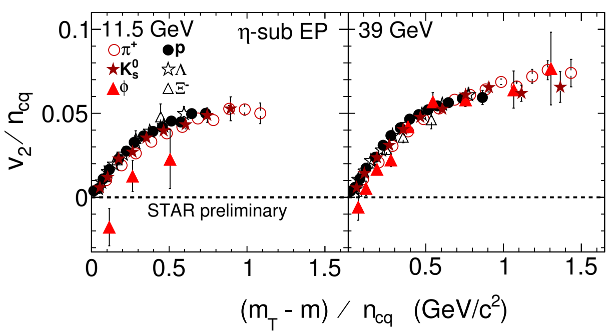

Fig. 5. v_2 scaled by the number of constituent quarks (n_{cq}) as a function of $m_{\mathrm{T}} - m$ over n_{cq} for various particles in Au+Au collisions. Please see [25] for more details.

Furthermore, the difference of v_2 between particles and antiparticles is found to be weakly dependent on energy from the $\sqrt{s_{NN}} = 39$ GeV on, while it shows a significant deviation at energies lower than $\sqrt{s_{NN}} = 11.5$ GeV (Fig. 6 (left panel)), which increases with decreasing energy [25].

Another interesting effect of a deviation at small energies is observed in the proton and antiproton slope dv_1/dy' of the v_1 flow coefficient of the protons and antiprotons at mid-rapidity as a function of beam energy at $\sqrt{s_{NN}} = 11.5$ GeV below which the proton slope changes sign, while the antiproton slope remains negative [26].

Furthermore, STAR has measured dynamical fluctuations of several particle ratios on an event-by-event basis in BES searching for a possible critical point. The K/π dynamical fluctuations from STAR show no significant energy dependence in Au+Au collisions from $\sqrt{s_{NN}} = 7.7$ to 200 GeV [27, 28].

Another remarkable result has been achieved by STAR while measuring the higher moments (variance σ^2, skewness S and kurtosis κ) of net-proton distributions in search for the QCD critical point. In particular, the

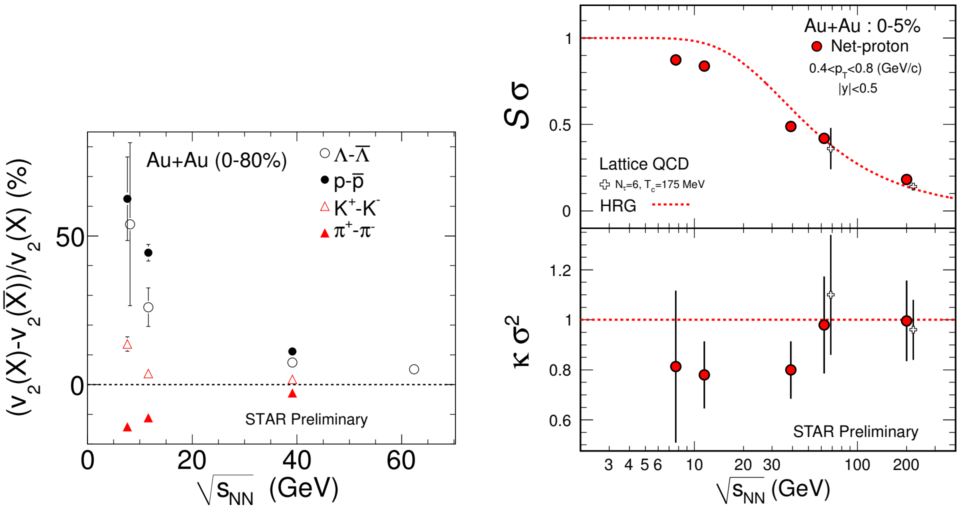

Fig. 6. Left panel: The difference of v_2 for particles and antiparticles divided by the particle v_2 as a function of collision energy in Au+Au collisions. Right panel: Energy dependence of moment products ($\kappa\sigma^2$ and $S\sigma$) of net-proton distributions for 0–5% most central Au+Au collisions. The dashed (red) lines denote the HRG model calculations, and the empty markers denote Lattice QCD results.

moment products $\kappa\sigma^2$ and $S\sigma$ of net-proton distributions in most central Au+Au collisions (Fig. 6 (right panel)) are consistent with Lattice QCD and Hadron Resonance Gas (HRG) model calculations between $\sqrt{s_{NN}} = 62.4$ and 200 GeV, while the results are smaller than the HRG model estimates at lower energies (at $\sqrt{s_{NN}} = 7.7$, 11.5, 39 GeV) [29, 30].

5. Conclusions and outlook

The STAR experiment at RHIC has entered a new era of high precision and high statistics measurements with the help of recent major upgrades, in particular, the addition of a barrel TOF detector, a Data Acquisition upgrade and a High Level Trigger. The highly enhanced data statistics and the new identification capabilities lead to a number of new striking results. STAR studies the properties of the new state of matter discovered at RHIC, the strongly interacting quark-gluon plasma measuring $A + A$ collisions at the top RHIC energy and accessing low baryochemical potential of about 20 MeV. Furthermore, STAR is exploring the QCD phase structure searching for a possible critical point and the phase boundary performing a beam energy scan with Au+Au collisions. New upgrades coming up, in particular the silicon Heavy Flavour Tracker detector (HFT) and the Muon Telescope

Detector (MTD), heading to data taking in 2014 will allow for high precision measurements of open heavy flavour, quarkonia and dimuon pairs towards significant discoveries in the coming years.

REFERENCES

[1] Yifei Zhang *et al.* [STAR Collab.], *J. Phys. G* **38**, 124142 (2011).
[2] H. Agakishiev *et al.* [STAR Collab.], *Phys. Rev.* **D83**, 052006 (2011).
[3] W. Li [STAR Collab.], *Acta Phys. Pol. B Proc. Suppl.* **5**, 413 (2012).
[4] M.M. Aggarwal *et al.* [STAR Collab.], *Phys. Rev. Lett.* **105**, 202301 (2010).
[5] Zebo Tang *et al.* [STAR Collab.], *J. Phys. G* **38**, 124107 (2011).
[6] B. Abelev *et al.* [STAR Collab.], *Phys. Rev.* **C80**, 041902 (2009).
[7] B. Wyslouch *et al.* [CMS Collab.], *J. Phys. G* **38**, 124005 (2011).
[8] X. Dong, *Acta Phys. Pol. B* **43**, 545 (2012) this issue.
[9] H. Qiu [STAR Collab.], *Acta Phys. Pol. B Proc. Suppl.* **5**, 323 (2012).
[10] R. Reed *et al.* [STAR Collab.], *J. Phys. G* **38**, 124185 (2011).
[11] L. Kosarzewski [STAR Collab.], *Acta Phys. Pol. B Proc. Suppl.* **5**, 543 (2012).
[12] B. Trzeciak [STAR Collab.], *Acta Phys. Pol. B Proc. Suppl.* **5**, 549 (2012).
[13] H. Satz, *J. Phys. G* **32**, R25 (2006).
[14] CMS Collaboration, *Phys. Rev. Lett.* **107**, 052302 (2011).
[15] H. Agakishiev *et al.* [STAR Collab.], *Nature* **473**, 353 (2011).
[16] B. Huang [STAR Collab.], *Acta Phys. Pol. B Proc. Suppl.* **5**, 471 (2012).
[17] M. Wada [STAR Collab.], *Acta Phys. Pol. B Proc. Suppl.* **5**, 249 (2012).
[18] M.M. Aggarwal *et al.* [STAR Collab.], `arXiv:1007.2613v1 [nucl-ex]`.
[19] O.I. Mall [STAR Collab.], *Acta Phys. Pol. B Proc. Suppl.* **5**, 491 (2012).
[20] X. Zhu [STAR Collab.], *Acta Phys. Pol. B Proc. Suppl.* **5**, 213 (2012).
[21] Lokesh Kumar *et al.* [STAR Collab.], *J. Phys. G* **38**, 124145 (2011).
[22] A. Andronic *et al.*, *Nucl. Phys.* **A772**, 167 (2006).
[23] X. Zhang [STAR Collab.], *Acta Phys. Pol. B Proc. Suppl.* **5**, 509 (2012).
[24] Md. Nasim [STAR Collab.], *Acta Phys. Pol. B Proc. Suppl.* **5**, 317 (2012).
[25] S. Shi [STAR Collab.], *Acta Phys. Pol. B Proc. Suppl.* **5**, 311 (2012).
[26] Y. Pandit [STAR Collab.], *Acta Phys. Pol. B Proc. Suppl.* **5**, 439 (2012).
[27] J. Tian [STAR Collab.], *Acta Phys. Pol. B Proc. Suppl.* **5**, 503 (2012).
[28] T.J. Tarnowski [STAR Collab.], *Acta Phys. Pol. B Proc. Suppl.* **5**, 515 (2012).
[29] X. Luo [STAR Collab.], *Acta Phys. Pol. B Proc. Suppl.* **5**, 497 (2012).
[30] S. Gupta *et al.*, *Science* **332**, 1525 (2011).